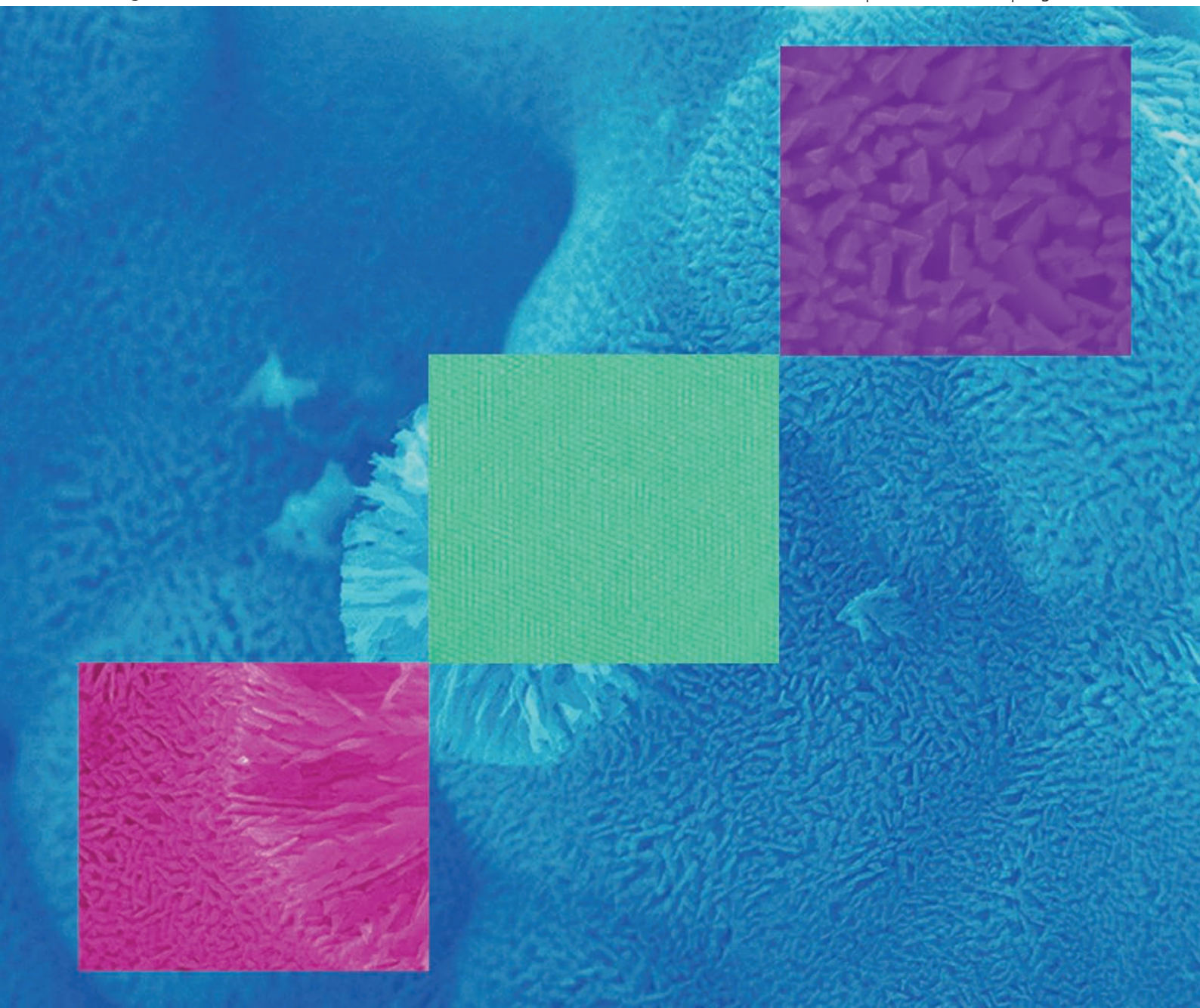


# ChemComm

Chemical Communications

[www.rsc.org/chemcomm](http://www.rsc.org/chemcomm)

Number 40 | 28 October 2007 | Pages 4061–4176



ISSN 1359-7345

**FEATURE ARTICLE**

Nagao Kobayashi and Katsunori Nakai  
Applications of magnetic circular  
dichroism spectroscopy to porphyrins  
and phthalocyanines

**COMMUNICATION**

Xiaosheng Fang *et al.*  
Si nanowire semisphere-like ensembles  
as field emitters



1359-7345(2007)40;1-3

RSC Publishing

# Si nanowire semisphere-like ensembles as field emitters

Xiaosheng Fang,\* Yoshio Bando, Changhui Ye, Guozhen Shen, Ujjal K. Gautam, Chengchun Tang and Dmitri Golberg

Received (in Cambridge, UK) 24th January 2007, Accepted 17th May 2007

First published as an Advance Article on the web 1st June 2007

DOI: 10.1039/b701113j

Silicon nanowires assembled in micro-sized semispheres were synthesized through simple thermal evaporation without using any templates and metal particle catalysts; electron microscopy revealed that the nanowires within semisphere ensembles are well-aligned and evenly distributed; a typical nanowire array density was of  $\sim 4 \times 10^9 \text{ cm}^{-2}$ ; field-emitting characteristics of the arrays were analyzed.

One-dimensional (1D) nanomaterials and nanostructures have attracted much interest in the past decade because of their novel physical properties and potential applications in constructing nanoscale electric and optoelectronic devices.<sup>1–4</sup> Silicon is the most important semiconducting and electronic material whose micro-electronics development was one of the greatest industrial successes of the 20th century. Many works were focused on the preparation of 1D Si nanowires, nanobelts, nanoribbons and nanotubes, using various methods, and utilization of Si nanostructures in miniaturized electronic devices exhibiting quantum confinement effects.<sup>5–7</sup> Novel properties of 1D Si nanomaterials and nanostructures, such as enhanced photothermal effect,<sup>8</sup> excellent field emission,<sup>9</sup> and photovoltaic applications<sup>10</sup> were discovered. Si nanowire arrays have been synthesized through adopting various templates or catalysts and using lithography.<sup>11</sup> However, the lithography techniques are expensive and template removal is difficult, and catalytic metal particles may become electron and hole traps in Si. This posed a serious contamination problem for Si complementary metal oxide semiconductor (CMOS) processing.<sup>12</sup>

Here, we describe the synthesis and analysis of dense Si semisphere-like ensembles composed of numerous nanowires. The nanomaterial was fabricated through simple thermal evaporation without usage of any templates or metal catalysts. All nanowires within semispheres were well-aligned. A typical nanowire array density was  $\sim 4 \times 10^9 \text{ cm}^{-2}$ . As produced Si nanostructures possess a turn-on field of  $\sim 7.3 \text{ V } \mu\text{m}^{-1}$  and a field enhancement factor of  $\sim 424$ .

Si nanostructure arrays were synthesized *via* thermal evaporation. A quartz crucible containing a ground mixture of Si (0.28 g) and SiO (0.44 g) powders was placed in the center of a quartz tube within a tube furnace. A long alumina plate was placed subsequently inside the reaction chamber to collect a product. 0.20 g activated carbon was placed in the downstream side of the furnace, where the temperature was  $\sim 600 \text{ }^\circ\text{C}$ . The tube furnace was purged with high-purity argon for 3 h prior to heating. The system was heated to  $1080 \text{ }^\circ\text{C}$  in 10 min and kept at this

temperature for 1 h, and then cooled to room temperature. The whole process was carried out under a constant flow of high-purity Ar at a rate of 100 sccm.

The collected products were characterized by a field-emission scanning electron microscope (SEM, JSM-6700F) and a powder X-ray diffractometer (XRD, RINT 2200HF, Cu-K $\alpha$  radiation).

Fig. 1(a) shows a SEM image of a product. Evenly distributed micro-sized semispheres are visible. An XRD pattern from the product is shown in Fig. 1(b). All diffraction peaks can be indexed to diamondlike cubic silicon (JCPDS file: 27–1402). The intensity of the (111) diffraction peak is much higher than the other peaks, indicating that the constituting Si nanostructures have a preferential orientation along the [111] direction.

Fig. 2 depicts SEM images of Si nanostructures taken at different viewing angles. Fig. 2(a) and (b) are the top views at high-magnification. These clearly reveal that the semispheres are composed of Si nanowire arrays. The nanowires have diameters in the range of 20–50 nm (with an average diameter of  $\sim 40 \text{ nm}$ ). Partially broken domains may be found in semispheres, as shown in Fig. 2(b). Fig. 2(c) is a cross-sectional SEM image, showing that all constituting Si nanowires are well-aligned and straight, and

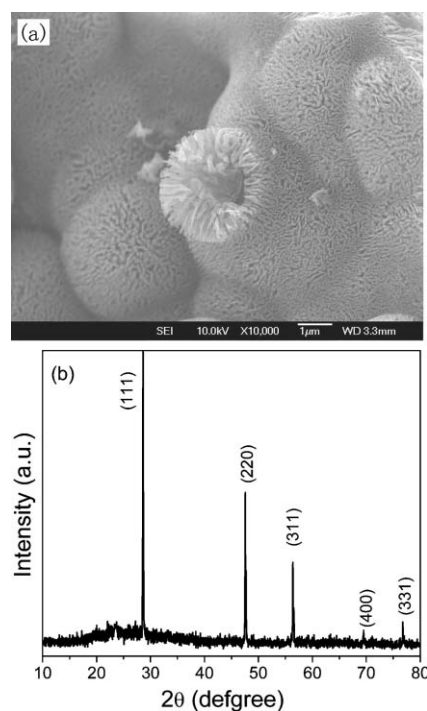
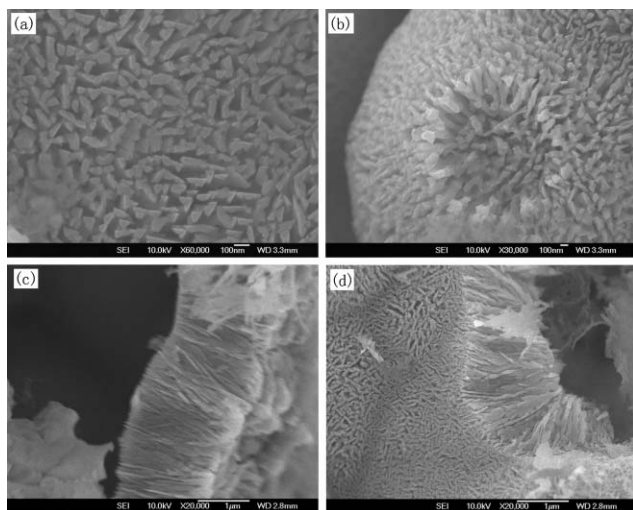


Fig. 1 (a) SEM image and (b) XRD pattern of a Si semisphere-like morphology product.

Nanoscale Materials Center, National Institute for Materials Science, Namiki 1-1, Tsukuba, Ibaraki, 305-0044, Japan.  
E-mail: Fang.Xiaosheng@nims.go.jp; Fax: (+81) 29-851-6280



**Fig. 2** SEM images of Si semisphere ensembles taken at different viewing angles. (a) and (b) Top-surface SEM images; (c) cross-sectional SEM image; and (d) an inclined image displaying both the top-surface and cross-sectional images showing inclined constituting Si nanowires.

have a length of  $\sim 2 \mu\text{m}$ . Interestingly enough, the present well-aligned nanostructures resemble those produced during the template-based growth.<sup>13</sup> One can clearly see both the top-surface and cross-section of Si ensembles in Fig. 2(d). Typically, the nanowire array density within a semisphere was of  $\sim 4 \times 10^9 \text{ cm}^{-2}$ .

A JEM-3000F high-resolution transmission electron microscope (HRTEM) equipped with an X-ray energy-dispersive spectrometer was used to further characterize the microstructures and their compositions. The typical low- and high-magnification TEM images are shown in Fig. 3(a) and 3(b). A TEM image confirms

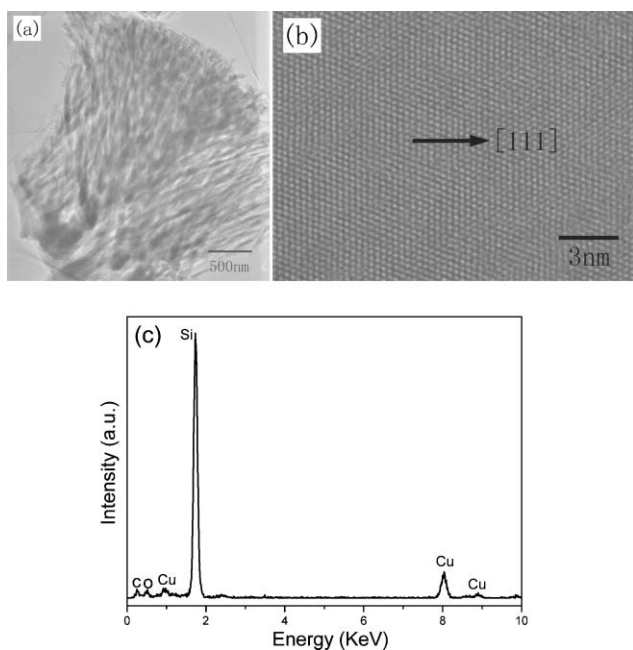


**Fig. 3** (a) TEM image of Si nanostructures; (b) and (c) a lattice-resolved HRTEM image, and EDS spectrum, respectively, taken from an individual nanowire.

that a semisphere consists of the Si nanowire arrays. HRTEM image verifies that these arrays are structurally uniform and composed of single crystalline wires. The resolved lattice spacing of  $\sim 0.31 \text{ nm}$  corresponds to the (111) lattice planes, indicating that the Si nanowire grew along the [111] orientation. This is in an agreement with the present XRD analysis and the general growth kinetics.<sup>14</sup> EDS spectra taken from a single nanowire [Fig. 3(c)] shows that the novel nanostructures are composed of Si with some marginal traces of oxygen.

There are several mechanisms that have been proposed to account for the growth of 1D nanomaterials and nanostructures by thermal evaporation method, including vapor–liquid–solid (VLS),<sup>15</sup> vapor–solid (VS),<sup>2</sup> and oxide-assisted mechanisms.<sup>16</sup> The VLS mechanism could be ruled out here because no metal catalyst was used in our experiments and no alloy particles were observed at the wire tips. We suggest that an oxide-assisted mechanism might dominate the growth of the present unusual structures. This assumption is based on the pre-existing systematic experiments and detailed analyses.<sup>16</sup> First, some Si or Si sub-oxide nanoclusters are deposited on the substrate through the decomposition of SiO under temperature increase. These nanoclusters densely cover the substrate. This was indeed confirmed by the SEM and TEM images taken from the nanostructure bottom portions. Then the clusters act as nuclei that absorb incoming Si vapor, which is continuously generated at a relatively high temperature under the Si powder evaporation, and transported to the nuclei. The diameter of the Si wires/islands is increasing while the array density is gradually decreasing, and finally the semisphere-like ensembles are formed. It should also be emphasized here that the role of activated C is to keep the deficiency of oxygen within the system atmosphere. It is worth noting that more work is underway to better understand the growth mechanism and to prepare other interesting Si or semiconductor nanostructures.

It is well known that aligned nanowires with a high density can enhance the material field-emission (FE) properties.<sup>17</sup> FE measurements on the as-synthesized product were conducted in a vacuum chamber at a pressure of  $4.6 \times 10^{-6} \text{ Pa}$  at room temperature. A rodlike aluminium probe of  $1 \text{ mm}^2$  cross section was used as an anode and a Si nanostructure film served as a cathode. A dc voltage sweeping from 100 to 1100 V was applied to a sample.<sup>18</sup> Fig. 4 shows the FE current density,  $J$ , as a function of the applied field,  $E$ , for a  $J$ - $E$  plot [Fig. 4(a)] and a  $\ln(J/E^2) - (1/E)$  plot [Fig. 4(b)] measured at anode–cathode distances of 100 and 120  $\mu\text{m}$ . The relatively smooth and consistent curves indicate the stability of emission from the Si nanostructure emitters. From Fig. 4, the turn-on field at a current density of  $10 \mu\text{A cm}^{-2}$  was extrapolated to be  $\sim 7.3 \text{ V } \mu\text{m}^{-1}$ . This value is significantly lower than those for many other Si emitter types, such as Si cone arrays ( $13$ – $16.5 \text{ V } \mu\text{m}^{-1}$ ),<sup>19</sup> Si nanowires ( $13 \text{ V } \mu\text{m}^{-1}$ ),<sup>20</sup> and single crystalline-Si microtips ( $15 \text{ V } \mu\text{m}^{-1}$ ).<sup>21</sup>

The field emission current–voltage characteristics can be expressed by a simplified Fowler–Nordheim equation,<sup>17,22</sup>

$$J = (A\beta^2 E^2 / \phi) \exp(-B\phi^{3/2} / \beta E) \text{ or}$$

$$\ln(J/E^2) = \ln(A\beta^2 / \phi) - B\phi^{3/2} / \beta E;$$

where  $A = 1.54 \times 10^{-6} \text{ A eV V}^{-2}$ ,  $B = 6.83 \times 10^3 \text{ eV}^{-3/2} \text{ V } \mu\text{m}^{-1}$ ,  $\beta$  is the field-enhancement factor, which is related to the geometry,

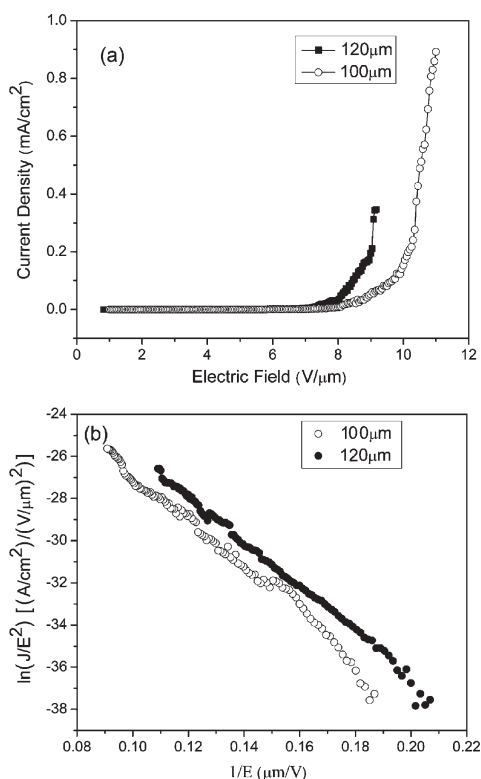


**Fig. 4** Field-emission properties of Si semisphere ensembles recorded at anode-cathode distances of 100 and 120  $\mu\text{m}$ . (a)  $J$ - $E$  curve, showing a turn-on field of  $\sim 7.3 \text{ V } \mu\text{m}^{-1}$  at a current density of  $10 \mu\text{A cm}^{-2}$ . (b) Fowler-Nordheim plot corresponding to (a).

crystal structure, and nanostructure density; and  $\phi$  is the work function of the emitting material, which is 3.6 eV for Si. The nearly linear plots in Fig. 4(b) indicate that the field emission from the Si semisphere ensembles is controlled by a barrier tunneling quantum-mechanical process. The enhancement factor  $\beta$  was calculated to be  $\sim 424$  from the slope of the fitted straight line in Fig. 4(b).

In summary, numerous micro-sized semisphere ensembles composed of Si nanowire arrays were successfully synthesized through simple thermal evaporation without using of any templates and metal catalysts. The nanowires within semispheres are well-aligned and uniformly distributed. A nanowire density within the arrays is typically of  $\sim 4 \times 10^9 \text{ cm}^{-2}$ . The turn-on field for field-emission of the arrays was  $\sim 7.3 \text{ V } \mu\text{m}^{-1}$ , which is significantly low compared to many previously reported Si nanostructure arrays.<sup>19-21</sup> The field enhancement factor  $\beta$  was measured as  $\sim 424$ . The present low-cost and straightforward method could be employed to synthesize many other new interesting Si (or other semiconductor) arrays/ensembles valuable for nanoscale electric and optoelectronic devices.

This work was financially supported by the Japan Society for the Promotion of Science (JSPS) fellowship tenable at the National

Institute for Materials Science, Tsukuba, Japan (X. S. F.). The authors thank Ms E. Arisumi, Drs Y. Uemura, M. Mitome, and C. Y. Zhi for cooperation and kind help.

## Notes and references

- 1 Y. N. Xia, P. D. Yang, Y. G. Sun, Y. Y. Wu, B. Mayers, B. Gates, Y. D. Yin, F. Kim and H. Q. Yan, *Adv. Mater.*, 2003, **15**, 353; X. S. Fang and L. D. Zhang, *J. Mater. Sci. Technol.*, 2006, **22**, 1; X. S. Fang and L. D. Zhang, *J. Mater. Sci. Technol.*, 2006, **22**, 721.
- 2 Z. W. Pan, Z. R. Dai and Z. L. Wang, *Science*, 2001, **291**, 1947.
- 3 X. S. Fang, C. H. Ye, L. D. Zhang and T. Xie, *Adv. Mater.*, 2005, **17**, 1661; X. S. Fang, C. H. Ye, L. D. Zhang, J. X. Zhang, J. W. Zhao and P. Yan, *Small*, 2005, **1**, 422; X. S. Fang, C. H. Ye, L. D. Zhang, Y. H. Wang and Y. C. Wu, *Adv. Funct. Mater.*, 2005, **15**, 63.
- 4 M. Nath and B. A. Parkinson, *Adv. Mater.*, 2006, **18**, 1865; C. L. Chen, D. R. Chen, X. L. Jiao and C. Q. Wang, *Chem. Commun.*, 2006, 4632.
- 5 Y. F. Zhang, Y. H. Tang, N. Wang, D. P. Yu, C. S. Lee, I. Bello and S. T. Lee, *Appl. Phys. Lett.*, 1998, **72**, 1835; J. D. Holmes, K. P. Johnston, R. C. Doty and B. A. Korgel, *Science*, 2000, **287**, 1471.
- 6 Y. Cui, L. J. Lauhon, M. S. Gudiksen, J. F. Wang and C. M. Lieber, *Appl. Phys. Lett.*, 2001, **78**, 2214; G. Audoit, T. Ni Mhuircheartaigh, S. M. Lipson, M. A. Morris, W. J. Blau and J. D. Holmes, *J. Mater. Chem.*, 2005, **15**, 4809.
- 7 S. M. Liu, M. Kobayashi and K. Kimura, *Chem. Commun.*, 2005, 4690; J. D. Carter, Y. Q. Qu, R. Porter, L. Hoang, D. J. Masiel and T. Guo, *Chem. Commun.*, 2005, 2274.
- 8 N. Wang, B. D. Yao, Y. F. Chan and X. Y. Zhang, *Nano Lett.*, 2003, **3**, 475.
- 9 C. Mu, Y. X. Yu, W. Liao, X. S. Zhao, N. S. Xu, X. H. Chen and D. P. Yu, *Appl. Phys. Lett.*, 2005, **87**, 113104; B. Q. Zeng, G. Y. Xiong, S. Chen, S. H. Jo, W. Z. Wang, D. Z. Wang and Z. F. Ren, *Appl. Phys. Lett.*, 2006, **88**, 213108.
- 10 K. Q. Peng, Y. Xu, Y. Wu, Y. J. Yan, S. T. Lee and J. Zhu, *Small*, 2005, **1**, 1062.
- 11 X. Y. Zhang, L. D. Zhang, G. W. Meng, G. H. Li, N. Y. J. Phillipp and F. Phillipp, *Adv. Mater.*, 2001, **13**, 1238; J. C. She, S. Z. Deng, N. S. Xu, R. H. Yao and J. Chen, *Appl. Phys. Lett.*, 2006, **88**, 013112; Y. K. Choi, J. Zhu, J. Grunes, J. Bokor and G. A. Somorjai, *J. Phys. Chem. B*, 2003, **107**, 3340.
- 12 Y. W. Wang, V. Schmidt, S. Senz and U. Gösele, *Nat. Nanotechnol.*, 2006, **1**, 186.
- 13 L. Li, Y. W. Yang, X. H. Huang, G. H. Li and L. D. Zhang, *J. Phys. Chem. B*, 2005, **109**, 12394; L. Li, Y. W. Yang, G. H. Li and L. D. Zhang, *Small*, 2006, **2**, 548; L. Li, G. H. Li, Y. Zhang, Y. W. Yang and L. D. Zhang, *J. Phys. Chem. B*, 2005, **108**, 109380.
- 14 S. P. Ge, K. L. Jiang, X. X. Lu, Y. F. Chen, R. M. Wang and S. S. Fan, *Adv. Mater.*, 2005, **17**, 56.
- 15 R. S. Wagner and W. C. Ellis, *Appl. Phys. Lett.*, 1964, **4**, 89.
- 16 N. Wang, Y. H. Tang, Y. F. Zhang, C. S. Lee, I. Bello and S. T. Lee, *Chem. Phys. Lett.*, 1999, **299**, 237; R. Q. Zhang, Y. Lifshitz and S. T. Lee, *Adv. Mater.*, 2003, **15**, 635.
- 17 A. Wei, X. W. Sun, C. X. Xu, Z. L. Dong, M. B. Yu and W. Huang, *Appl. Phys. Lett.*, 2006, **88**, 213102.
- 18 Y. B. Li, Y. Bando, D. Golberg and K. Kurashima, *Appl. Phys. Lett.*, 2002, **81**, 5048.
- 19 N. G. Shang, F. Y. Meng, F. C. K. Au, Q. Li, C. S. Lee, I. Bello and S. T. Lee, *Adv. Mater.*, 2002, **14**, 1308.
- 20 F. C. K. Au, K. W. Wong, Y. H. Tang, Y. F. Zhang, I. Bello and S. T. Lee, *Appl. Phys. Lett.*, 1999, **75**, 1700.
- 21 T. Sugino, S. Kawasaki, K. Tanioka and J. Shirafuji, *Appl. Phys. Lett.*, 1997, **71**, 2704.
- 22 Y. F. Lin, Y. J. Hsu, S. Y. Lu and S. C. Kung, *Chem. Commun.*, 2006, 2391; W. Z. Wang, B. Q. Zeng, J. Yang, B. Poudel, J. Y. Huang, M. J. Naughton and Z. F. Ren, *Adv. Mater.*, 2006, **18**, 3275.